ACS APPLIED MATERIALS & INTERFACES

RESEARCH ARTICLE

www.acsami.org

Polarization and Electric Field Dependence of Electronic Properties in $LaAlO_3/SrTiO_3$ Heterostructures

Xiaoping Yang and Haibin Su*

Division of Materials Science, Nanyang Technological University, 50 Nanyang Avenue, 639798 Singapore

ABSTRACT: We have done the detailed theoretical investigation by performing calculations for numerous $LaAlO_3/SrTiO_3$ heterostructures using the generalized gradient approximation. We find that external electric field can cooperate or compete with spontaneous polarization and effectively modulate band dispersion around the Fermi level. Positive field can induce a reversible insulator−metal transition in insulating heterostructures. Rather than the Ti-d_{xy} interface state that emerges in insulator−metal transition without external field, the pd-σ anti-bonding state composed of the O-p_z and the Ti-d_{3z^2-1} at $SrTiO_3$ surface exchanges its hole with the electron of the O-p_xp_y orbitals (bonding states) at $LaAlO_3$ surface with the presence of positive field. Associated with insulator−metal transition, there is a remarkable change of local work functions in heterostructure, which suggests that $LaAlO_3/SrTiO_3$ heterostructures are the promising candidates for novel nanoscale oxide electronic devices and technology, for instance, the Schottky diodes with adjustable barrier height.

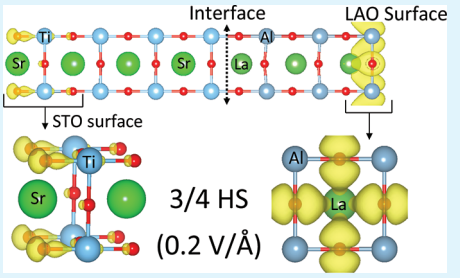

KEYWORDS: oxide heterostructures, density functional calculation, electronic structure, atomic polarization, insulator−metal transition, electric field effect

INTRODUCTION

Transition metal oxides exhibit a huge variety of intrinsic functionalities such as magnetism, superconductivity, thermoelectricity, ferroelectricity or multiferroic behavior.[1−26] Experimentally, there is also growing interest in the creation of "oxide heterostructures" consisting of alternating layers of different transition−metal oxides.[2,3] Oxide−oxide interfaces often give rise to novel physical phenomena not exhibited in the bulk constituents, due to the rearrangement of charge, spins, orbitals, lattice and the resulting rebalancing of their mutual interactions. Thus interface can be exploited to modify electronic structure and to tailor novel properties and behaviors.

Recently, much effort has been made for *n*-type heterointerface (TiO_2/LaO) between two insulating perovskites, the polar $LaAlO_3$ (LAO) and nonpolar $SrTiO_3$ (STO), in both theoretic and experimental work.[4−20] But the origin of the new complex phases (metallic states,[4,5] magnetism,[6] and even superconductivity[7]) emerging at the LAO/STO interface has not been completely resolved yet, due to the fact that these phases result from a combination of different mechanisms,[8] *e.g.*, electronic interface reconstruction, structural deformations, and oxygen vacancies. Even experimentally Thiel et al.[5] have found that the insulator-to-metal transition can also be induced dynamically by an external electric field. Which kind of mechanism dominates the behavior in a given sample appears to be sensitive to the conditions under which the sample is grown and/or how it is processed prior to the experimental measurements. So far, one important theoretical progress shows that superlattice structure cannot model the experimental configuration completely, where the AlO_2 surface is exposed to vacuum. As discussed in refs 19 and 20, the existence of surface has a profound effect on the physical properties of heterostructures observed experimentally.

Herein, we shed light on polarization and external electric field dependence of electronic properties in ideal LAO/STO heterostructure (HS) with *n*-type interface, as illustrated in Figure 1. Our studies show that LAO/STO heterostructures are on the verge of energy instability due to spontaneous polarized potential across LAO part, and the combination of intrinsic polarized potential and external electric field can enhance or weaken band shift, even lead to a reversible insulator−metal transition in insulating heterostructure. Associated with this transition, there is the remarkable change of local work function.

RESULTS AND DISCUSSION

We took the lattice constant of bulk $SrTiO_3$ (3.905 Å)[25] as the in-plane lattice constant *a* of *n*(LAO)/*m*(STO) heterostructure (these will be abbreviated by *n*/*m* HS in the following text) ($3 \leq n, m \leq 5$, see the top panel of Figure 1). Therefore, the Ti−O and Al−O distance in the *x* − and *y* −directions became 1.9525 Å, not far from the value in bulk $LaAlO_3$.[27] The *z* coordinates of atoms were relaxed except for the lowest STO layer fixed for simulating substrate effect. The main effect of the relaxation, shown in the bottom panel of Figure 1, is to make the negatively charged O and positively charged cations displaced relative to each other and polarize the cation and anion planes. In both LAO and STO parts, non-superficial oxygen atoms always dimple towards the interface. Only oxygen atoms in superficial AlO_2

Received: February 15, 2011
Accepted: September 20, 2011
Published: September 20, 2011

dx.doi.org/10.1021/am201115r | *ACS Appl. Mater. Interfaces* 2011, 3, 3819–3823

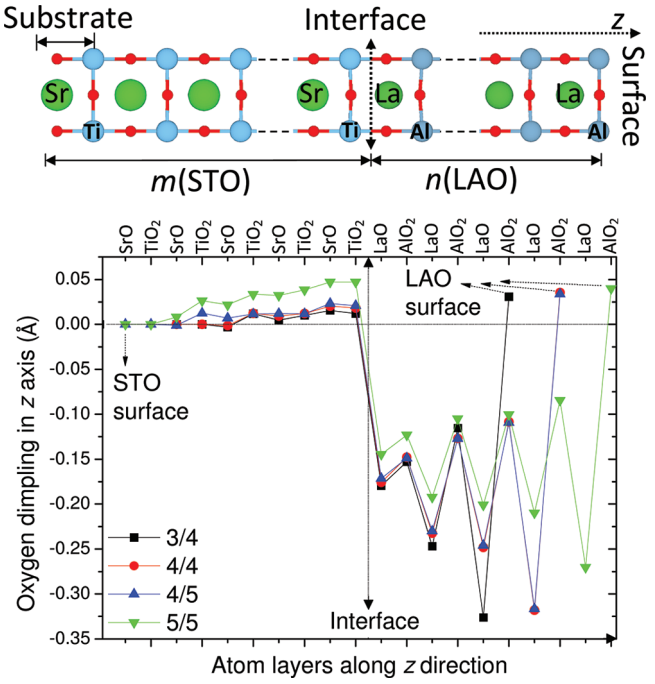

Figure 1. Top panel: Schematic geometrical structures of n(LAO)/m(STO) heterostructure ($3 \le n, m \le 5$). Bottom panel: Calculated oxygen dimpling away from cation planes in the z direction.

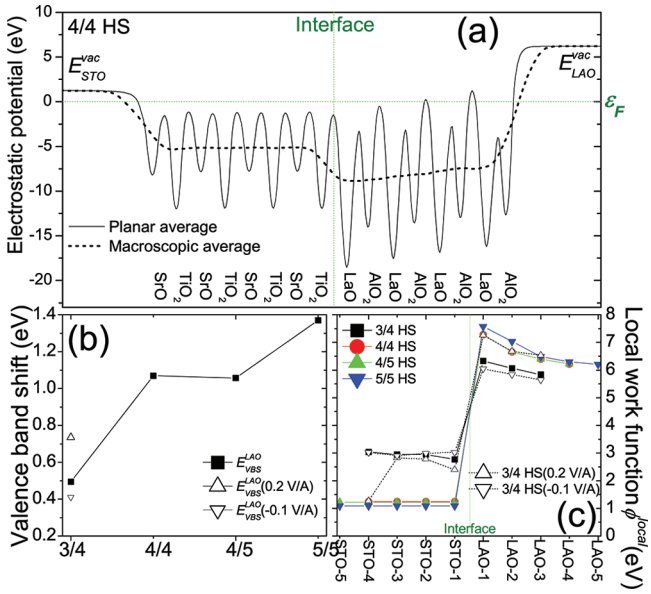

Figure 2. (a) Planar average and macroscopic average of the electrostatic potential for metallic 4/4 heterostructure. Valence band shift E_{VBS}^{LAO} of LAO part (b) and local work function ϕ^{local} (c) for n(LAO)/m(STO) heterostructure obtained by layer projected density-of-state and electrostatic potential calculations. The results obtained for 3/4 HS at −0.1 and 0.2 V/Å field are also plotted in (b) and (c) for comparison.

plane move slightly towards vacuum. Atomic polarization occurs mostly in the LAO part, and the largest cation-anion polarization of LaO planes is about 0.33 Å and much close to surface, and non-superficial AlO_2 planes have the largest polarization of 0.15 Å at interface. This polarization distortion pointing to interface produces a local ionic dipole moment, and also leads to an increase in the out-of-plane Ti−Ti distance by about 0.07 Å at interface. All these results are much different with those obtained for LAO/STO superlattice where atomic polarization is predominantly in STO part.[16]

Local ionic dipole moment arouses inevitably an internal polarized electric field across LAO part of heterostructure. To illustrate clearly how the polar field reduces the energy gap, we show in Figure 2a the planar averaged electrostatic potential[28] and its macroscopic average (MA) along the z direction perpendicular to the interface and surface for metallic 4/4 heterostructure. As the figure shows, the MA potential of STO is almost flat, indicating that there is no internal electric field through the STO. In the LAO part, the MA potential is increasing layer by layer, which eventually upshifts the valence band edge of LAO surface layer over the Fermi level. The valence band shift (VBS) of the LAO part is defined as the difference between the valence band edges of the LAO layers at surface and interface, i.e., $E_{VBS}^{LAO} = E_V^{LAO-S} - E_V^{LAO-I}$. As we can see in Figure 2b, E_{VBS}^{LAO} increases with the increasing thickness of LAO part. Based on the E_{VBS}^{LAO} values of metallic 4/5 and 5/5 heterostructures, we estimate internal electric field is 82.6 mV/Å, consistent with the experimentally observed value of 80.1 mV/Å.[9]

An evolution of surface states (O-p) and interface states (Ti-d) can be clearly observed in band structures of heterostructures without electric field. Figure 3 shows the energy bands of n(LAO)/m(STO) heterostructure in a 5 eV region around the Fermi level $\varepsilon_F \equiv 0$ and along the symmetry lines Γ-X-M-Γ = (0,0,0) − ((π/a),0,0) − ((π/a),(π/a),0) − (0,0,0). The 3/4 HS without electric field has a 0.56 eV indirect gap above the filled O-2p bands, and below the unfilled Ti-3d bands. Ti-3d bands have their minimum at Γ point, and O-2p bands have their maximum at M point. Because of the deformed geometry structure and the quantum confinement from finite size effect, the high degeneracy of original bulk Ti-3d bands is lifted and the band splitting occurs in heterostructure. With the increasing thickness of LAO, one can find that Ti-3d and O-2p bands shift close to each other, resulting in an insulator−metal transition observed experimentally at the critical number of $n = 4^5$ (4/4 or 4/5 HS). The lowest Ti-3d band exchanges its hole with the electron of the toppest O-2p band. The changing of layer number of STO from 4 to 5 almost has no effect on energy bands, which indicates that 4 or 5 layers STO is thick enough to give a reasonable description for physical properties of heterostructure. Going then to the 5/5 heterostructure, more Ti-3d conduction bands take part in this transition due to the increased polarized potential, which enhances the metallic behavior of system.

To investigate the physical origin of insulator−metal transition, we plot the charge density of the occupied bands of 4/5 HS from -0.2 eV to the Fermi level in Figure 4a. Obviously, insulator−metal transition originates from charge transfer between Ti-d_{xy} orbitals at interface and O-p_x,p_y at LAO surface, coinciding with the trend of band structures in Fig. 3. This result is similar to that of Pentcheva et al.,[19] although the LAO/STO HSs studied in their paper are capped with additional STO layers on LAO surface. Here, Ti-d_{xy} bands are lower than the Ti-d_{xz},d_{yz} bands because of the larger in-plane hopping integrals. Interestingly, the occupied Ti-d_{xy} states do not locate only at interface but spread several layers into STO part. Based on analysis for wave function characters, we find that these occupied states actually are a linear combination of Ti-d_{xy} from different TiO_2 planes. For heterostructures with 4 layers LAO, the only occupied Ti-d_{xy} state is mainly localized in the interfacial TiO_2

plane, and wave function character decays away from the interface. When the layer number of LAO is increased to five, the wave function character of Ti-d_{xy} is enhanced in non-interfacial TiO_2 planes.

Motivated by recent experimental observation,[5] in which external electric field was used to mimic the effect of dipole polarization, we investigate the effect of perpendicular electric fields in the z direction considering the crucial role of dipole moment in insulator−metal transition. It can be anticipated that the external electric field, cross not only LAO but also STO part, will cooperate or compete with spontaneous polarization, and the enhanced or weakened band shift will occur, and therefore resulting in a subtle change of electronic structure. Simulations for insulating 3/4 heterostructure reveal the charge-dependent effect of applied external electric fields in the range of −0.1 to 0.2 V/Å illustrated in Figure 5. Applied positive field gradually reduces the energy gap at 0.1 V/Å, meantime a O−Ti pd-σ anti-bonding band (see label in Figure 5) downshifts and much close to the Fermi level. Finally, this pd-σ band overlaps with O-p band at the Fermi level, and directly drives an insulator−metal transition at 0.2 V/Å. On the other hand, a negative field of −0.1 V/Å is found to enlarge the band gap to 1.18 eV. These results confirm the crucial role of the polarized potential in insulator−metal transition, and indicates that the insulating HSs are well suited to generate and control a quasi-two-dimensional electron gas by electric field effect. To illustrate charge transfer mechanism at 0.2 V/Å, we plot the charge density of the occupied bands from −0.11 eV to the Fermi level in Figure 4b. Obviously, it is not Ti-d_{xy} interface state (exists in metallic HSs without external field, see Figure 4a) to exchange its hole with the electron of O-p_xp_y at LAO surface, but the pd-σ anti-bonding state composed of O-p_z and Ti-d_{3z^2-1} at STO surface. The forming of this surface state results from the introduced external field in STO part, which inevitably leads to an additional potential gradient and modifies electronic structure of STO part.

The layer-projected densities-of-states in Figure 6 show that the potential increment at LAO surface is not large enough to overcome the band gap of STO for 3/4 HS, and the system remains insulating. In 4/4 heterostructure, the increased LAO thickness promotes the potential increment which is larger than the band gap of STO, so that the Ti-d_{xy} states of STO part and O-p_xp_y states of LAO-surface meet each other at the Fermi level. However, an additional positive 0.2 V/Å electric field cooperates with spontaneous polarization and drives an insulator−metal transition in 3/4 HS. On the contrary, negative 0.1 V/Å field competes with spontaneous polarization and increases energy gap to 1.18 eV. In Figure 6, the band edge shifts from layer to layer in LAO part indicating an electric field discontinuity consistent with the accumulation of a positive monopole charge at interface or STO surface in metallic phase. Electrons attracted to this monopole reside on the STO side, as already confirmed from the partial charge density plot (Figure 4). From Figure 2b,

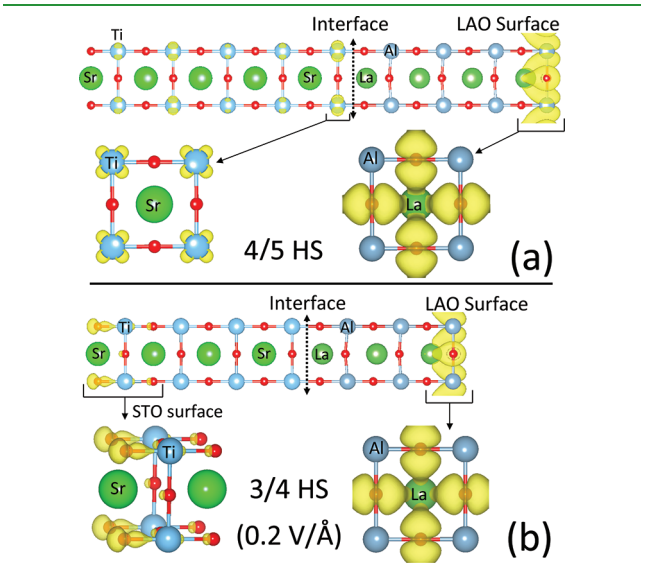

Figure 4. Partial charge density isosurfaces for the occupied bands (a) from −0.2 eV to the Fermi level for 4/5 HS, and (b) from −0.11 eV to the Fermi level for 3/4 HS.

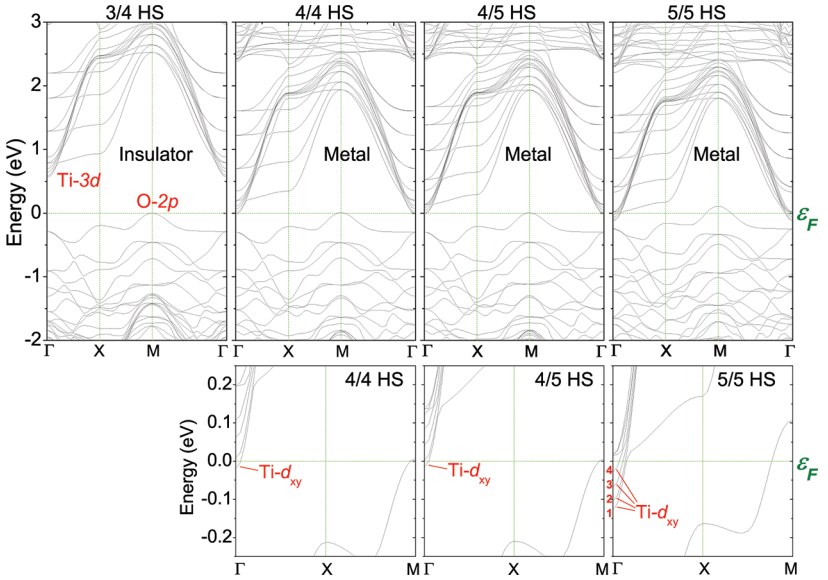

Figure 3. GGA bandstructures of n(LAO)/m(STO) heterostructures. The Fermi level ε_F is set at zero. The bottom three panels show the band structures around ε_F of metallic 4/4, 4/5, and 5/5 HSs in an enlarged energy scale.

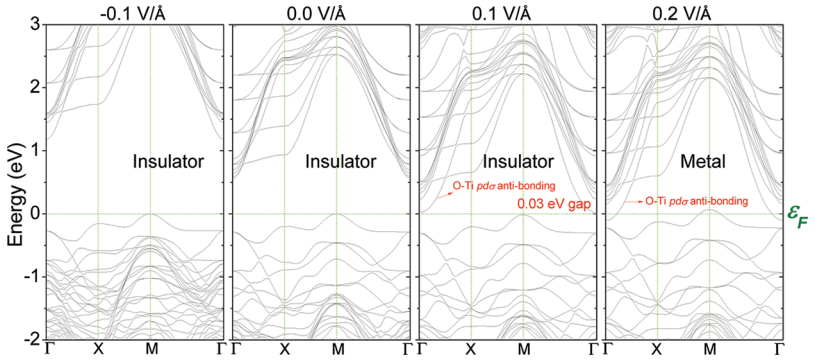

Figure 5. GGA bandstructures of 3/4 heterostructure with the applied electric fields in the modulus of -0.1− 0.2 V/Å along the z direction (see Fig. 1). The Fermi level ε_F is set at zero.

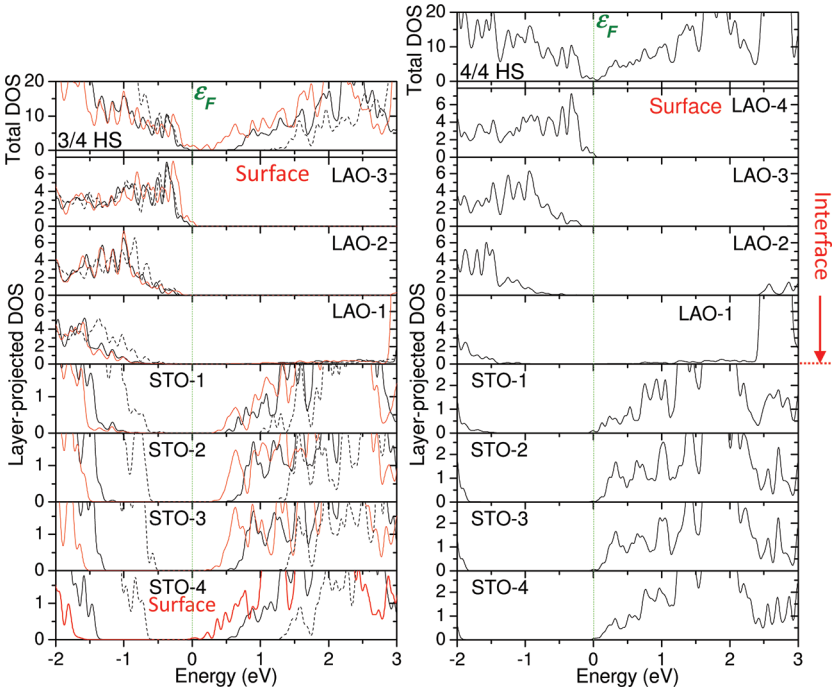

Figure 6. Layer projected density of states of insulating 3/4 (left panel) and metallic 4/4 (right panel) heterostructures. Here, black solid lines are for HS without external field, and black dash (red solid) line is for 3/4 HS at −0.1(0.2) V/Å, respectively.

we can find that E_{VBS}^{LAO} value depends on not only geometry structure of heterostructures but also external field. In the case of 3/4 HS, the −0.1 V/Å field decreases E_{VBS}^{LAO} to 0.410 eV, and the 0.2 V/Å field increases E_{VBS}^{LAO} to 0.735 eV.

What is also worth noticing is local work function ϕ^{local} (see Figure 2c) defined by $\phi^{local} = E_{STO(LAO)}^{vac} - \varepsilon_F^{local}$, where $E_{STO(LAO)}^{vac}$ is vacuum energy level of STO or LAO part, as shown in Figure 2a, and ε_F^{local} is local Fermi level of every STO(LAO) layer in layer projected density of states. For all heterostructures with or without external field, local work function of LAO part decreases layer by layer from interface to surface because of the polarized potential. With the increased LAO thickness n or introducing of positive external field, local work function at interface ϕ_{LAO-1}^{local} is increasing, and ϕ_{STO-1}^{local} is just the reverse. Both of them have an remarkable change by +0.962 and −1.515 eV at n = 4 for HS without external field, respectively, associating with an insulator−metal transition in electronic structures. Comparing local work functions of metallic 5/5 HS to those of metallic 4/5 HS, we find that the variation at n = 5 from change of LAO thickness is +0.297 eV for LAO-1 and −0.134 eV for STO-1, much smaller than above mentioned changes at n = 4. For metallic heterostructures, this means the forming of an adjustable Schottky diodes. Especially, for 3/4 HS with external field at 0.2 V/Å (see black uptriangle and dash line in Figure 2c), the change of local work function, associated with insulator−metal transition, is mainly reflected at STO surface, rather than conventionally observed interface. The reason is that electric field is applied across not only LAO but also STO part, which results in the appearance of a new STO surface state.

CONCLUSIONS

In conclusion, we have reported the detailed ab initio simulation for n-type LAO/STO heterostructures. We have demonstrated

how the polarized potential of LAO part overcomes the band gap of STO, making O-p_x, p_y bands at surface overlap with Ti-d_{xy} bands at interface, and how external electric field cooperates or competes with spontaneous polarization and effectively modulates band dispersion around the Fermi level, even induces a reversible insulator−metal transition in insulating heterostructure. Most interestingly, we find the O−Ti pd-σ state at STO surface plays the critical role in the insulator−metal transition under external electric field. Furthermore, our calculations reveal a significant change of local work function in heterostructure associated with insulator−metal transition triggered by either electric field effect or pure spontaneous polarization from LAO part. Our studies indicate that $LaAlO_3/SrTiO_3$ heterostructures are the promising candidates for novel nanoscale oxide electronic devices and technology, e.g., metal-semiconductor junction in Schottky diodes, and even 2D electron gas based memory devices. Also, the intrinsic physical mechanism revealed in our paper can be applied to other oxide heterostructures with extended surface and intrinsic polarization.

THEORETICAL METHODS AND MODELS

We carried out the numerical calculations using the Vienna ab initio Simulation Package (VASP)[29−32] within the framework of generalized gradient approximation (GGA) (Perdew-Burke-Ernzerhof exchange correlation functional).[33,34] The ion-electron interaction was modeled by the projector augmented wave (PAW) method[35,36] with a uniform energy cutoff of 500 eV. For heterostructure, we used periodic boundary conditions and a vacuum layer thick enough to prohibit the out-of-plane electronic and dipole−dipole interactions between neighboring heterostructures. Spacing between k points was 0.02 $Å^{-1}$. The geometry structures of heterostructures were optimized by employing the conjugate gradient technique, and in the final geometry, no force on the atoms exceeded 0.01 eV/Å. Because of the well-known insufficient of density functional methods to describe excited states, the magnitude of the band gap is underestimated systematically. The calculated values for bulk STO and LAO are 2.0 and 3.7 eV (experimental measurement 3.3 and 5.6 eV), respectively.

AUTHOR INFORMATION

Corresponding Author
*E-mail: hbsu@ntu.edu.sg.

ACKNOWLEDGMENT

This work was supported in part by a MOE AcRF-Tier-1 grant (no. M52070060) and A*STAR SERC grant (M47070020).

REFERENCES

(1) Vashaee, D.; Shakouri, A. *Phys. Rev. Lett.* **2004**, *92*, 106103–106106.
(2) Izumi, M.; Ogimoto, Y.; Konishi, Y.; Manako, T.; Kawasaki, M.; Tokura, Y. *Mater. Sci. Eng. B* **2001**, *84*, 53–57.
(3) Ohtomo, A.; Muller, D. A.; Grazul, J. L.; Hwang, H. Y. *Nature* **2002**, *419*, 378–380.
(4) Ohtomo, A.; Hwang, H. Y. *Nature* **2004**, *427*, 423–426.
(5) Thiel, S.; Hammerl, G.; Schmehl, A.; Schneider, C. W.; Mannhart, J. *Science* **2006**, *313*, 1942–1945.
(6) Brinkman, A.; Huijben, M.; van Zalk, M.; Huijben, J.; Zeitler, U.; Maan, J. C.; van der Wiel, W. G.; Rijnders, G.; Blank, D. H. A.; Hilgenkamp, H. *Nat. Mater.* **2007**, *6*, 493–496.
(7) Reyren, N.; Thiel, S.; Caviglia, A. D.; Kourkoutis, L. F.; Hammerl, G.; Richter, C.; Schneider, C. W.; Kopp, T.; Rüetschi, A.-S.; Jaccard, D.; Gabay, M.; Muller, D. A.; Triscone, J.-M.; Mannhart, J. *Science* **2007**, *317*, 1196–1199.
(8) Huijben, M.; Brinkman, A.; Koster, G.; Rijnders, G.; Hilgenkamp, H.; Blank, D. H. A. *Adv. Mater.* **2009**, *21*, 1665–1677.
(9) Singh-Bhalla, G.; Bell, C.; Ravichandran, J.; Siemons, W.; Hikita, Y.; Salahuddin, S.; Hebard, A. F.; Hwang, H. Y.; Ramesh, R. *Nat. Phys.* **2011**, *7*, 80–86.
(10) Bert, J. A.; Kalisky, B.; Bell, C.; Kim, M.; Hikita, Y.; Hwang, H. Y.; Moler, K. A. *Nat. Phys.* doi:10.1038/nphys2079.
(11) Pentcheva, R.; Pickett, W. E. *Phys. Rev. B* **2008**, *78*, 205106–205110.
(12) Park, M. S.; Rhim, S. H.; Freeman, A. J. *Phys. Rev. B* **2006**, *74*, 205416–205421.
(13) Albina, J. M.; Mrovec, M.; Meyer, B.; Elsässer, C. *Phys. Rev. B* **2007**, *76*, 165103–165114.
(14) Janicka, K.; Velev, J. P.; Tsymbal, E. Y. *Phys. Rev. Lett.* **2009**, *102*, 106803–106806.
(15) Zhong, Z.; Kelly, P. J. *EPL* **2008**, *84*, 27001–27005.
(16) Popović, Z. S.; Satpathy, S.; Martin, R. M. *Phys. Rev. Lett.* **2008**, *101*, 256801–256804.
(17) Lee, J.; Demkov, A. A. *Phys. Rev. B* **2008**, *78*, 193104–193107.
(18) Chen, H.; Kolpak, A.; Ismail-Beigi, S. *Phys. Rev. B* **2010**, *82*, 085430–085449.
(19) Pentcheva, R.; Huijben, M.; Otte, K.; Pickett, W. E.; Kleibeuker, J. E.; Huijben, J.; Boschker, H.; Kockmann, D.; Siemons, W.; Koster, G.; Zandvliet, H. J. W.; Rijnders, G.; Blank, D. H. A.; Hilgenkamp, H.; Brinkman, A. *Phys. Rev. Lett.* **2010**, *104*, 166804–166807.
(20) Son, W.-J.; Cho, E.; Lee, B.; Lee, J.; Han, S. *Phys. Rev. B* **2009**, *79*, 245411–245417.
(21) Chakhalian, J.; Preeland, J. W.; Srajer, G.; Strempfer, J.; Khaliullin, G.; Cezar, J. C.; Charlton, T.; Dalgliesh, R.; Bernhard, C.; Cristiani, G.; Habermeier, H.-U.; Keimer, B. *Nat. Phys.* **2006**, *2*, 244–248.
(22) Chakhalian, J.; Preeland, J. W.; Habermeier, H.-U.; Cristiani, G.; Khaliullin, G.; van Veenendaal, M.; Keimer, B. *Science* **2007**, *318*, 1114–1117.
(23) Yang, X.; Yaresko, A. N.; Antonov, V. N.; Andersen, O. K. *Condens. Matter* **2009**No. arXiv:0911.4349.
(24) Hansmann, P.; Yang, X.; Toschi, A.; Khaliullin, G.; Andersen, O. K.; Held, K. *Phys. Rev. Lett.* **2009**, *103*, 016401–016404.
(25) Hansmann, P.; Toschi, A.; Yang, X.; Andersen, O. K.; Held, K. *Phys. Rev. B* **2010**, *82*, 235123–235130.
(26) Benckiser, E.; Haverkort, M. W.; Brück, S.; Goering, E.; Macke, S.; Fraó, A.; Yang, X.; Andersen, O. K.; Cristiani, G.; Habermeier, H.; Boris, A. V.; Zegkinoglou, I.; Kim, H. J.; Hinkov, V.; Keimer, B. *Nat. Mater.* **2011**, *10*, 189–193.
(27) Zhu, J.; Zheng, L.; Zhang, Y.; Wei, X. H.; Luo, W. B.; Li, Y. R. *Mater. Chem. Phys.* **2006**, *100*, 451–456.
(28) Baldereschi, A.; Baroni, S.; Resta, R. *Phys. Rev. Lett.* **1988**, *61*, 734–737.
(29) Kresse, G.; Hafner, J. *Phys. Rev. B* **1993**, *47*, 558–561.
(30) Kresse, G.; Hafner, J. *Phys. Rev. B* **1994**, *49*, 14251–14269.
(31) Kresse, G.; Furthmüller, J. *Phys. Rev. B* **1996**, *54*, 11169–11186.
(32) Kresse, G.; Furthmüller, J. *Phys. Rev. B* **1996**, *6*, 15–50.
(33) Ceperley, D. M.; Alder, B. J. *Phys. Rev. Lett.* **1980**, *45*, 566–569.
(34) Perdew, J. P.; Burke, K.; Ernzerhof, M. *Phys. Rev. Lett.* **1996**, *77*, 3865–3868.
(35) Kresse, G.; Joubert, D. *Phys. Rev. B* **1999**, *59*, 1758–1775.
(36) Blöchl, P. E. *Phys. Rev. B* **1994**, *50*, 17953–17979.

NOTE ADDED AFTER ASAP PUBLICATION

This paper was published on the Web on October 6, 2011, with a minor error in reference 16, due to a production error. The corrected version was reposted on October 11, 2011.